Washington University in St. Louis
Washington University Open Scholarship

Biology Faculty Publications & Presentations　　　　　　　　　　Biology

2012

A pre-embedding immunogold approach reveals localization of myosin VI at the ultrastructural level in the actin cones that mediate Drosophila spermatid individualization

Marta Lenartowska
Nicolaus Copernicus University of Torun

Mamiko Isaji
Washington University in St Louis

Kathryn G. Miller
Washington University in St Louis

Follow this and additional works at: https://openscholarship.wustl.edu/bio_facpubs

Part of the Biology Commons

A pre-embedding immunogold approach reveals localization of myosin VI at the ultrastructural level in the actin cones that mediate *Drosophila* spermatid individualization

Marta Lenartowska[*]**, Mamiko Isaji, Kathryn G. Miller**

Marta Lenartowska[*]

Laboratory of Developmental Biology, Institute of General and Molecular Biology, Faculty of Biology and Earth Sciences, Nicolaus Copernicus University, Gagarina 9, 87-100 Toruń, Poland, phone: (56) 611 4997, Fax: (56) 611 4772, e-mail: mlenart@umk.pl

[*]Corresponding author

Mamiko Isaji

Department of Biology, Washington University in St. Louis, Campus Box 1137, 1 Brookings Dr., St. Louis, MO 63130, US

Kathryn G. Miller

Department of Biology, Washington University in St. Louis, Campus Box 1137, 1 Brookings Dr., St. Louis, MO 63130, US

1

Abstract

Stable actin structures play important roles in the development and specialization of differentiated cells. How these structures form, are organized, and are used to mediate physiological processes is not well understand in most cases. In *Drosophila* testis, stable actin structures, called actin cones, mediate spermatid individualization, a large-scale cellular remodeling process. These actin cones are composed of two structural domains, a front meshwork and a rear region of parallel bundles. Myosin VI is an important player in proper actin cone organization and function. Myosin VI localizes to the cones' fronts and its specific localization is required for proper actin cone formation and function during individualization. To understand how these structures are organized and assembled, ultrastructural studies are important to reveal both organization of actin and the precise localization of actin regulators relative to regions with different filament organizations. In the present work we have developed a novel pre-embedding immunogold-silver labeling method for high-resolution analysis of protein distribution in actin structures which allowed both satisfactory antibody labeling and good ultrastructural preservation. Electron microscopic studies revealed that myosin VI accumulated at the extreme leading edge of the actin cone and preferentially localized throughout the front meshwork of the cone where branched actin filaments were most concentrated. No myosin VI labeling was found adjacent to the membranes along the length of the cone or connecting neighboring cones. This method has potential to reveal important information about precise relationships between actin-binding proteins, membranes, and different types of actin structures.

Keywords

Abbreviations

BSA – bovine serum albumin

EM – electron microscopy

JLA20 – anti-actin antibody

MAb – monoclonal antibody

PB – phosphate buffer

PBS – phosphate-buffered saline

Introduction

Actin structures take a variety of forms in different cell types. These structures are often stable features of cells that persist over long periods of time and play important roles in cell and tissue organization and physiology. How such structures form and are organized and maintained is not well understood in most cases. One important step in understanding such structures is revealing the precise organization of actin in them and the relationship between those filaments and proteins that help organize and stabilize the actin structures. Localization of actin-associated proteins has been studied in many such structures at the light microscope level. However, few studies have shown structure organization in sufficient detail to resolve precise filament organization and relationship between those actin filaments and the proteins that are important to generate and maintain that organization (for some examples see Asano et al. 2001; Stromer et al. 2002; Furness et al. 2005; Marchelletta et al. 2008). Although such information can only be gathered by ultrastructural studies, preservation and visibility of actin filament structure and simultaneous immunolocalization for actin-associated proteins is difficult. Conditions required for good preservation and visualization of actin often preclude antibody labeling for a variety reasons. In this work, we developed a method for such localization using a model system, *Drosophila* spermatid individualization, which is amenable to functional manipulation actin binding protein activity. Combining ultrastructural information about actin organization with high resolution localization of actin-associated proteins under conditions in which we manipulate protein function will help us understand the formation and function of these structures.

Stable actin structures play an important role during a late step of *Drosophila* spermatogenesis, called spermatid individualization. During individualization, a cyst of 64 syncytial spermatids is reorganized into individual mature sperm by membrane remodeling and removal of cytoplasmic contents (Tokuyasu et al. 1972; Fabrizio et al. 1998; Noguchi and Miller 2003). This cellular remodeling is driven by long-lived actin structures called actin cones which travel synchronously along the axonemes from the sperm nuclei to the ends of the tails. The membrane of the cyst is remodeled to enclose each sperm separately. The bulk of the cytoplasm and most organelles are excluded from the individualized spermatids, accumulate in the cystic bulge ahead of the cones and are finally excluded from mature sperm as the waste bag. Previously, we demonstrated that the actin cones are composed of two main

domains, a rear region of parallel bundles and a front region of dense meshwork, which are differentially regulated and have different functions (Noguchi et al. 2006, 2008). The bundles are required for cone movement and the meshwork serves a structural role, acting like a bulldozer to exclude the cytoplasm and organelles from the sperm tails. One of the proteins that play a key role in maintaining the proper actin organization in the cones is myosin VI. Myosin VI localizes to the cones' fronts and promotes formation of a dense actin meshwork that grows larger as the cones move (Hicks et al. 1999; Noguchi et al. 2006). In myosin VI mutants, the cones do not accumulate sufficient F-actin, resulting in disruption of their movement before individualization is completed (Noguchi et al. 2006). Moreover, cellular components that are normally eliminated from mature sperm are no longer excluded. Instead, a large amount of cytoplasm remains and some groups of sperm tails are not properly separated by plasma membranes, resulting in male sterility. Myosin VI is also required for proper localization of some actin-binding proteins known to have roles in regulation of actin dynamics (Rogat and Miller 2002; Noguchi et al. 2008). The absence of myosin VI results in impaired distribution of these regulators, suggesting that myosin VI may stabilize the actin cone structure by coordinating the localization of specific actin binding proteins. These findings led us to propose a structural role for myosin VI in *Drosophila* spermatid individualization. However, its precise mechanism of action in this process remains unclear.

Myosin VI is a ubiquitously expressed unconventional actin-based molecular motor, which converts energy from ATP hydrolysis into mechanical force. Myosin VI is the only known actin-based motor that moves toward the pointed (minus or slow growing) end of an actin filament, the opposite direction from other characterized myosins (Wells et al. 1999; Ménétrey et al. 2005). The altered structure that mediates backward motility also confers other unusual properties. Under high backward load the movement of myosin VI stalls, and the protein behaves as an anchor, attaching cargos and/or adaptors to actin (Altman et al. 2004; Chuan et al. 2011). These atypical properties of myosin VI suggest that this motor protein may have unique cellular functions that are based on its anchoring role (Frank et al. 2004; Sweeney and Houdusse 2007, 2010).

In this report we carried out an ultrastructural analysis of actin and myosin VI distribution in actin cones. Electron microscopic observations of myosin VI in these highly specialized actin structures has not been previously described. Two different immunocytochemical methods and some modifications of these methods were tested. We show here that a modified pre-embedding immunogold labeling proved to be the best for

4

precise analysis of myosin VI distribution and potentially other important proteins, in actin cones.

Materials and Methods

Fly husbandry and primary culture of cysts

D. melanogaster were raised on standard cornmeal, agar, and sucrose medium at room temperature. Oregon R was used as the wild-type strain. In vitro culture of elongated cysts isolated form testes dissected from newly enclosed adult males was carried out as previously described (Cross and Shellenbarger 1979; Noguchi and Miller 2003). For this study, individualizing cysts with the cystic bulge positioned between one-fourth and one-third of the cyst length were used.

Conventional electron microscopy (EM)

For ultrastructural analysis of actin cones in cystic bulges, isolated individualizing cysts were washed twice with 0.1 M phosphate-buffered saline (PBS), pH 7.0. After washing, each cyst was stuck on a small piece of plastic sheet coated with poly-L-lysine (Thermanox, Electron Microscopy Sciences) by pushing on both sides of the cystic bulge with a thin glass needle. This step allowed the cyst to remain in one plane for later longitudinal sectioning of the actin cones present inside the cystic bulge. The cysts were then fixed with 1.5 % glutaraldehyde (EM grade, Sigma) in PBS for 3 h on ice, washed three times with PBS, postfixed with 1 % osmium tetroxide (OsO_4, Sigma) for 1 h at 4°C, and finally were brought to room temperature and rinsed twice with PBS before processing for EM. The samples were dehydrated through an ethanol series, infiltrated and embedded in Poly/Bed 812 resin using a standard protocol (Polysciences). Longitudinal sections of the cystic bulges (60-70 nm) were cut using a diamond knife (Micro Star Technologies) and a Leica UTC ultramicrotome. Ultrathin sections were stained with 2.5 % uranyl acetate and 0.4 % lead citrate solutions, and examined using a JEOL EM 1010 transmission electron microscope.

Myosin II subfragment 1 (S1) fragment decoration

Purification of rabbit skeletal myosin II and preparation of S1 subfragment were carried out using standard methods (Margossian and Lowey 1982). To examine actin cone structure, individualized cysts were selected from cultures and processed for myosin S1 fragment

decoration and EM visualization using the procedures described previously (Noguchi et al. 2006, 2008).

Immunolabeling

Two methods were tested for immunocytochemical actin and myosin VI localizations on actin cones of individualizing cysts at the EM level: post-embedding and pre-embedding immunogold techniques.

For post-embedding immunogold actin localization, isolated individualizing cysts were washed twice with 0.1 M PBS, pH 7.0. After washing, cysts were stuck on small pieces of plastic sheet as described above. The cysts were then fixed with 4 % formaldehyde (EM grade, Polysciences) in PBS for 30 min. at room temperature, rinsed three times in PBS, dehydrated through an ethanol series, and finally infiltrated and embedded in LR White resin using a standard protocol (Electron Microscopy Sciences). During polymerization of the resin, the small pieces of plastic sheets with cysts stuck to them were put vertically inside gelatin capsules to enable cutting of longitudinal sections. Ultrathin sections were collected on nickel grids covered with 0.3 % Formvar (Sigma). Sections were incubated in blocking solution containing 2 % bovine serum albumin in PBS (BSA, Sigma) for 15 min. at room temperature. Next, sections were kept in 1:50 dilution of a primary, monoclonal mouse anti-actin antibody (JLA20 IgM MAb, Calbiochem) in PBS supplemented with 0.2 % BSA for 1 h and washed three times in PBS, followed by incubation with a secondary antibody (anti-mouse IgG/IgM 10 nm, Aurion) diluted 1:100 in PBS with 0.2 % BSA for 1 h at room temperature. The cysts were then washed three times with PBS, postfixed with 1 % glutaraldehyde in PBS for 5 min., and finally washed several times with PBS and mQ H_2O before staining. Sections were stained with 2.5 % uranyl acetate and examined using transmission electron microscopy.

For pre-embedding immunogold actin and myosin VI localization, isolated individualizing cysts were washed twice with 0.1 M PBS, pH 7.0. The cysts were then stuck on small pieces of plastic sheets as described above. To improve penetration of the labeling reagents, cell membranes were treated with 0.1 % saponin (Sigma) in PBS for 10 min. For some of the cysts the permeabilizing solution was supplemented with 20 μM phalloidin (Sigma). After washing twice in PBS, cysts were fixed with 4 % formaldehyde (EM grade, Polysciences) and 0.2 % tannic acid (Electron Microscopy Sciences) for 10 min. at room temperature, washed a few times with PBS, and then incubated in blocking solution containing 2 % BSA in PBS for 30 min. at room temperature. The primary mouse MAbs:

6

anti-actin JLA20 IgM or anti-myosin VI 3C7 IgG (Kellerman and Miller 1992) diluted 1:50 and 1:20 respectively in PBS with 0.2 % BSA was applied at room temperature for 2 h, followed by overnight incubation at 4°C. The next day, cysts were washed three times in PBS and incubated with secondary antibodies (ultra-small anti-mouse IgG/IgM 0.8 nm, Aurion) diluted 1:100 with PBS supplemented with 0.2 % BSA for 2 h at room temperature. The cysts were then washed with PBS and rinsed twice with sodium phosphate buffer (PB), pH 6.8, and fixed with 1.5 % glutaraldehyde (EM grade, Sigma) in PB for 30 min. at room temperature. After extensive washes in PB, mQ H_2O, and 0.02 M sodium citrate buffer, pH 7.0, the gold particles were amplified using a silver-enhancing kit (Aurion). Silver enhancing was stopped in mQ H_2O. Then the cysts were postfixed with 1 % OsO_4 for 30 min. at room temperature, and finally washed twice in mQ H_2O. The samples were dehydrated, embedded in Poly/Bed 812 (Polysciences), cut in longitudinal ultrathin sections, stained and examined under transmission electron microscope as described above for ultrastructural analysis.

Control samples were prepared according to the same protocols for post-embedding and pre-embedding immunogold localizations with exception of incubations with the primary antibodies.

Actin and myosin VI staining in actin cones at the light microscope level were examined using the methods described previously (Rogat and Miller 2002; Noguchi and Miller 2003).

Results

Ultrastructural analysis of actin cones in the individualizing cyst

In previous reports, two different methods of sample preparation for electron microscopy were used to examine the process of individualization: myosin II S1 decoration technique and conventional EM (Noguchi et al. 2006, 2008). While both methods revealed some similar features, each was more effective at resolving some features. Using rabbit skeletal muscle myosin II S1 subfragment decoration, it was possible to see actin filament organization. Myosin II S1 decoration is a standard method used to reveal the organization and orientation of actin filaments, because this protein fragment binds at a characteristic angle, making an arrowhead pattern along the filament length and causing filmants to appear thicker. In wild-type *Drosophila* males, fully elongated cysts undergoing individualization contained synchronously moving actin cones composed of two main domains: a rear region of

parallel bundles and a front dense meshwork. These different structural and functional domains are easily distinguishable in longitudinal sections of cones examined at the EM level (Fig. **1a-b** and previous reports). The myosin II S1 decoration method very clearly revealed that as the cones moved along the cyst their front meshwork became bigger and much more dense (compare Fig. **1a**, **b**). The myosin II S1 decoration technique did not preserve the cone membrane because of the relatively strong permeabilization and the decoration step on unfixed material that is required for this technique.

Conventional EM revealed different features. Each actin cone appears as a triangular grey fibrous area surrounded by individual smooth membrane (Fig. **1c-d**, arrowheads) which connected to the adjacent membranes of neighboring cones at the positions where these membranes appeared to form an inverted 'U' (Fig. **1c**, arrows). This connecting membrane is the place where the process of membrane remodeling is thought to occur during individualization. The F-actin organization present in the structural domains seen by myosin II S1 decoration was difficult to discern when the cysts were fixed according to this procedure. Although the precise actin organization was not clear, the front region of the actin cone contained significantly thicker fibrous material compared to the rear region (Fig. **1d**). These regions correspond to the dense actin meshwork and parallel bundles, respectively, visualized using myosin II S1 decoration (Fig. **1a-b**). Only application of both methods of EM observation allowed a detailed analysis of the individualizing cyst ultrastructure.

The pre-embedding immunogold method is better for antigen localization in actin cones

To understand the organization and relationship of myosin VI and actin to each other and the membrane, immunolocalization at the EM level was attempted. Two different methods, post-embedding and pre-embedding labeling, with a few additional technical modifications were tested. Actin localization was performed as a specific control in order to develop the best procedure for antibody penetration and reproducible results. The best technique was then used to detect myosin VI, while preserving the highly-organized actin cytoskeleton in these unique structures.

First, we examined standard post-embedding immunogold labeling of the isolated cysts using the relatively mild fixation (4 % formaldehyde) generally used for light level immunocytochemistry. This method revealed the expected actin distribution, along the whole length and width of the cones (Fig. **2b**), but the ultrastructural preservation of the filaments was highly unsatisfactory (Fig. **2a-b**). Despite the poor preservation, longitudinal sections of

the actin cones had the proper triangular shape and were surrounded by cone membranes (Fig. **2a**, small arrows). Axoneme/mitochondria pairs were visible inside the cones, but the distinct F-actin organization in the previously defined structural domains as revealed by myosin II S1 decoration was absolutely impossible to discern (Fig. **2a**). At higher magnification, some gold particles were localized adjacent to the cone membrane (Fig. **2b**, arrows). This result indirectly supports the idea that the cone membrane is tightly associated with the actin filaments as might be expected based on actin in other situations.

To try to simultaneously obtain both good immunolocalization of the antigen and well-preserved cone ultrastructure, a pre-embedding immunogold technique was next tested. Theoretically, this technique should make it possible to obtain suitable preservation of both features, because immunolabeling is performed prior to the strong fixation necessary for preservation of ultrastructure and subsequent embedding in the resin. This technique is therefore a powerful method for subcellular localization of proteins. Despite its advantages, pre-embedding immunolocalization has potentially one general limitation, like possible decreased penetration of immunoreagents even though cell membranes are permeabilized. In the case of individualizing cysts, immunoreagents need to penetrate through two layers, the somatic cyst cells that enclose the entire cyst and the membrane of the syncytial cysts themselves, which surrounds the nuclei, axoneme and actin cone of each spermatid.

Pre-embedding immunogold localization of actin carried out according to standard protocol on unfixed material and examined in longitudinal sections did not reveal the expected results. Despite the effective penetration of antibodies through the somatic cyst cells and spermatid membranes and proper binding to the epitopes, the actin cytoskeleton was partially disrupted (Fig. **3a-c**). Some empty spaces were visible in both the front and rear domains of the cone (Fig. **3a**, small arrows), suggesting that actin filaments were partially destroyed under the conditions of incubation. This undesirable outcome was not surprising since the actin cytoskeleton is a dynamic structure that can quickly undergo rearrangements or destruction in response to external stimuli, including chemical agents. However, a satisfactory level of labeling was present in small regions of the actin cone where the actin cytoskeleton was well preserved (Fig. **3b-c**), indicating that antibody penetration was excellent. Therefore, we modified the method to obtain better preservation of actin filaments by supplementing the permeabilizing solution with phalloidin, which stabilizes F-actin (Dancker et al. 1975). Additionally, after permeabilization we gently stabilized the cysts with 4 % formaldehyde and 0.2 % tannic acid, two fixatives recommended for immuno-cytochemistry. This modified

9

procedure of pre-embedding immunogold localization resulted in good preservation of the actin cytoskeleton and the expected actin distribution (Fig. **4a-c**). Inspection of longitudinal sections of the cones revealed uniform labeling of the two distinct actin organization regions - the dense actin meshwork at the front and the parallel bundles in the rear (Fig. **4a-b**). Moreover, axoneme/mitochondria pairs were visible inside the cones and membranes were sufficiently well preserved. At higher magnification, some gold-silver particles were localized adjacent to the cone membrane (Fig. **4c**, arrows) similar to results obtained using the post-embedding method. Control sections without primary antibody incubation did not reveal any specific labeling within the actin structures, except for a few randomly distributed background particles (data not shown). Taken together, we concluded that the modified pre-embedding immunogold method is suitable for detailed analysis of protein distribution in actin cones at the EM level.

Localization of myosin VI in actin cones during individualization at the EM level

In previous reports, we showed that in individualizing cysts myosin VI localized at the fronts of actin cones and this localization is required for the proper actin cone structure and actin content. In the absence of myosin VI, spermatid individualization was not properly completed and males were sterile (Hicks et al. 1999; Rogat and Miller 2002; Noguchi et al. 2006). In myosin VI mutants, other actin-binding proteins were disorganized. These findings led us to propose a structural role for myosin VI in *Drosophila* spermatogenesis, but verification of this hypothesis required knowing the precise localization of myosin VI. Immunofluorescence and GFP-myosin VI localization studies revealed that in moving actin cones, myosin VI localized as a tight band at the front of the cones (Fig. **5a-c** and previous reports). This localization of myosin VI was confirmed in this work at the EM level using the modified pre-embedding immunogold technique. Specific labeling was mainly found in the front meshwork (Fig. **6a-c**). As the cones moved along the cyst myosin VI was concentrated at the extreme leading edge of the actin cone (Fig. **6b**, arrows). However, a much-reduced concentration of gold-silver labeling was also visible in the rear domain of parallel actin bundles (Fig. **6a**). It was not so apparent using fluorescence microscopy. Longitudinal serial sections through the actin cones showed that myosin VI was not localized as a ring at the base of the cone but was present in the whole area filled with actin meshwork (data not shown). In this domain, label was localized preferentially in the regions where branched actin filaments were most concentrated

(Fig. **6b-c**). In the sections showing well-preserved cone membrane, labeling was not found directly at the membrane, as was seen when actin was localized. In addition, no gold-silver particles were detected adjacent to the membrane that connected neighboring cones (Fig. **6b-c**, double arrows). These data show that myosin VI is primarily associated with the F-actin forming the front meshwork, supporting its structural role in actin organization. The lack of labeling associated with the membranes suggested that this protein is not involved directly in the membrane remodeling which occurs during spermatid individualization. Control sections without primary antibody incubation did not reveal any specific labeling, except for a few randomly distributed background particles (Fig. **6d**).

Discussion

Some previous reports have shown immunocytochemical localization of myosin VI at the EM level using conventional post-embedding immunogold techniques. Most of them revealed the presence of this protein in the regions near the plasma and intracellular membrane structures such as Golgi complex, recycling endosome, and various vesicles involved in endocytosis and secretion or occurring in the active synaptic zone (Hasson et al. 1997; Buss et al. 2001; Warner et al. 2003; Rzadzinska et al. 2004; Morriswood et al. 2007; Sobczak et al. 2008; Roux et al. 2009; Puri et al. 2010). In these post-embedding experiments, the efficiency of labeling was satisfactory, but actin structures were not visible. Therefore, application of this technique was not suitable for the localization of proteins within the highly organized F-actin structures mediating spermatid individualization in *Drosophila*.

In the present study, a novel labeling technique was developed using ultra-small gold particles and a modified pre-embedding methodology to visualize localization of myosin VI in high-organized actin cones. Since the current protocol allowed us to combine selective immunolabeling with a good ultrastructural preservation, we could localize the distribution of myosin VI relative to the distinct structural domains of the cones. We are confident that the method we have developed results in labeling that reflects the actual myosin VI localization on actin cones for three reasons. We tested this method first for actin localization and compared pattern of labeling with a standard post-embedding technique. Actin labeling pattern was analogous using both methods, with uniform actin distribution over the whole cone and the presence of some labeling adjacent to the cone membrane. Second, our observations of myosin VI distribution using pre-embedding immunogold technique are in excellent general agreement with the results obtained in immunofluorescence and GFP-

myosin VI localization experiments. However, ultrastructural localization revealed an aspect of myosin VI localization which was not detected in light microscopic observations: that a small amount of signal was associated with the rear of the cones, in the region of parallel bundles. Finally, this new protocol preserves the actin cytoskeleton of the cone in a pattern similar to that produced by the myosin II S1 decoration technique. Thus, this method should be suitable for preserving actin structures and allowing immunolocalization relative to these structures in other contexts.

Based on our previous and present studies, we suggest that myosin VI acts as an anchor during spermatid individualization to stabilize actin cones, protecting the pointed ends of the filaments from depolymerizing factors (Noguchi et al. 2006) or by recruiting and tethering unidentified proteins or protein complexes necessary for regulation of actin dynamics at the fronts of the cones (Rogat and Miller 2002; Noguchi et al. 2006). Our present results demonstrate that either of these hypotheses might be valid. The specific gold-silver labeling indicates that as the cones move along the cyst and their front meshwork became bigger myosin VI is highly concentrated at the extreme leading edge of the actin cone. This specific myosin VI localization might reflect its possible accumulation near the minus ends of actin filaments, since we previously showed that most filaments are oriented with their pointed ends facing the front of the actin cone (Noguchi et al. 2006). Also, the unique ability of myosin VI to move toward the minus end of actin filament (Wells et al. 1999; Ménétrey et al. 2005) is consistent with a myosin VI translocation to extreme front of actin cone.

We showed here that in the front meshwork of functional actin cone myosin VI-immunoreactivity preferentially labeled regions where the dense meshwork of branched actin filaments were most concentrated. These areas are likely to be zones of active actin assembly. Some actin-binding proteins known to have important roles in regulation of actin assembly, such as the Arp2/3 actin nucleation complex and its activator, cortactin, also localized to the front domain of the actin cone (Rogat and Miller 2002; Noguchi et al. 2008). In myosin VI mutants, cones do not accumulate sufficient F-actin to exclude cytoplasmic contents during movement (Hicks et al. 1999; Noguchi et al. 2006) and asymmetric distribution of actin regulators is disrupted (Rogat and Miller 2002; Isaji et al. unpublished data). Thus, myosin VI could mediate recruitment to and retention of these and/or other important proteins at the fronts of actin cones in places where their activities are required. This idea is consistent with myosin VI's ablity to act as a load-dependent anchor in vitro (Altman et al. 2004). But so far none of the proteins that have been studied appear to be a direct partner of myosin VI during

12

spermatid individualization in *Drosophila.* However, the modified pre-embedding immunogold method described here offers the excellent possibility for studies of putative myosin VI interacting proteins to observe their precise localizations relative to myosin VI.

None of our present and previous data support the idea that myosin VI functions as a transporter involved in endo- or exocytosis during *Drosophila* spermatid individualization. Cellular reorganization during this process separates a cyst of 64 syncytial spermatids into individual sperm each surrounded by a single membrane. Myosin VI is at the extreme leading edge of the synchronously moving cones. This location places this protein in an ideal position to link sites of membrane remodeling to actin dynamics. We originally hypothesized this region might either be an area of high endocytic membrane trafficking or a region where newly synthesized membrane and cytoskeleton components are delivered. However, we could not see any myosin VI labeling adjacent to the membranes along the length of the cone or connecting neighboring cones. These results are constant with our previous reports, which provided no support for endo- or exocytosis activities around the actin cones (Rogat and Miller 2002; Noguchi and Miller 2003). Thus, myosin VI is unlikely to play a direct role in membrane remodeling.

This new pre-embedding method allows the simultaneous observation of antigen distribution, actin ultrastructure, membrane organization, and other features. The technique should be applicable to other types of actin structures and cell types. Revealing the precise relationships between actin regulatory proteins, motor cargoes, and different filament arrangements should increase our understanding of how the many different types of actin structure found in differentiated cells are formed, are maintained, and function.

Conflict of interest None.

References

13

Altman D, Sweeney HL, Spudich JA (2004) The mechanism of myosin VI translocation and its load-induced anchoring. Cell 116:737-749

Asano Y, Mabuchi I (2001) Calyculin-A, an inhibitor for protein phosphatases, induces cortical contraction in unfertilized sea urchin eggs. Cell Motil Cyto 48:245-261

Buss F, Arden SD, Lindsay M, Luzio JP, Kendrick-Jones J (2001) Myosin VI isoform localized to clathrin-coated vesicles with a role in clathrin-mediated endocytosis. EMBO J 20:3676–3684

Chuan P, Spudich JA, Dunn AR (2011) Robust mechanosensing and tension generation by myosin VI. J Mol Biol 405:105-112

Cross DP, Shellenbarger DL (1979) The dynamics of *Drosophila melanogaster* spermatogenesis in in vitro cultures. J Embryol Exp Morphol 53:345-351

Dancker P, Löw I, Hasselbach W, Wieland T (1975) Interaction of actin with phalloidin: polymerization and stabilization of F-actin. Biochim Biophys Acta. 400:407-14

Fabrizio JJ, Hime G, Lemmon SK, Bazinet C (1998) Genetic dissection of sperm individualization in *Drosophila melanogaster.* Development 125:1833-1843

Frank DJ, Noguchi T, Miller KG (2004) Myosin VI: a structural role in actin organization important for protein and organelle localization and trafficking. Curr Opin Cell Biol 16:189-194

Furness DN, Katori Y, Mahendrasingam S, Hackney CM (2005) Differential distribution of β- and γ-actin in guinea-pig cochlear sensory and supporting cells. Hear Res 207:22-34

Hasson T, Gillespie PG, Garcia JA, MacDonald RB, Zhao Y, Yee AG, Mooseker MS, Corey DP (1997) Unconventional myosins in inner-ear sensory epithelia. J Cell Biol 137:1287–1307

Hicks JL, Deng WM, Rogat AD, Miller KG, Bownes M (1999) Class VI unconventional myosin VI is required for spermatogenesis in *Drosophila*. Mol Biol Cell 10:4341-4353

Kellerman KA, Miller KG (1992) An unconventional myosin heavy chain gene from *Drosophila melanogaster.* J Cell Biol 119:823-834

Marchelletta RR, Jakobs DT, Schechter JE, Cheney RE, Hamm-Alvares SF (2008) The class V myosin motor, myosin 5c, localizes to mature secretory vesicles and facilitates exocytosis in lacrimal acini. Am J Physiol Cell Physiol 295:C13-C28

Margossian SS, Lowey S (1982) Preparation of myosin and its subfragments from rabbit skeletal muscle. Methods Enzymol 85B:55-71

14

Ménétrey J, Bahloul A, Wells AL, Yengo CM, Morris CA, Sweeney HL, Houdusse A (2005) The structure of the myosin VI motor reveals the mechanism of directionality reversal. Nature 435:779-785

Morriswood B, Ryzhakov G, Puri C, Arden SD, Roberts R, Dendrou C, Kendrick-Jones J, Buss F (2007) T6BP and NDP52 are myosin VI binding partners with potential roles in cytokine signaling and cell adhesion. J Cell Sci 120:2574-2585

Noguchi T, Lenartowska M, Miller KG (2006) Myosin VI stabilizes an actin network during *Drosophila* spermatid individualization. Mol Biol Cell 17: 2559-2571

Noguchi T, Lenartowska M, Rogat AD, Frank DJ, Miller KG (2008) Proper cellular organization during *Drosophila* individualization depends on actin structures composed of two domains, bundles and meshwork, that are differentially regulated and have different functions. Mol Biol Cell 19:2363-2372

Noguchi T, Miller KG (2003) A role of actin dynamics in individualization during spermatogenesis in *Drosophila melanogaster*. Development 130:1805-1816

Puri C, Chibalina MV, Arden SD, Kruppa A, Kendrick-Jones J, Buss F (2010) Overexpression of myosin VI in prostate cancer cells enhances PSA and VEGF secrecion, but has no effect on endocytosis. Oncogene 29:188-2000

Rogat AD, Miller KG (2002) A role for myosin VI in actin dynamics at sites of membrane remodeling during *Drosophila* spermatogenesis. J Cell Sci 115:4855-4865

Roux I, Hosie S, Johnson SL, Bahloul A, Cayet N, Nouaille S, Kros CJ, Petit C, Safieddine S (2009) Myosin VI is required for the proper maturation and function of inner hair cell ribbon synapses. Hum Mol Gen 18:4615-4628

Rzadzinska AK, Schneider ME, Davies C, Riordan GP, Kachar B (2004) An actin molecular treadmill and myosins maintain stereocilia architecture and self-renewal. J Cell Biol 164:887-897

Sobczak M, Wasik A, Kłopocka W, Rędowicz MJ (2008) Involvement of myosin VI immunoanalog in pinocytosis and phagocytosis in *Amoeba proteus*. Biochem Cell Biol 86:509-519

Stromer MH, Mayes MS, Bellin RM (2002) Use of actinisoform-specific antibodies to probe the domain structure in three smooth muscles. Histochem Cell Biol 118:291-299

Sweeney HL, Houdusse A (2007) What can myosin VI do in cells? Curr Opin Cell Biol 19:57-66

Sweeney HL, Houdusse A (2010) Myosin VI rewrites the rules for myosin motors. Cell 141:573-582

15

Tokuyasu KT, Peacock WJ, Hardy RW (1972) Dynamics of spermatogenesis in *Drosophila melanogaster*. I. Individualization process. Z Zelloforsch Mikrosk Anat 124:479-506

Warner CL, Stewart A, Luzio JP, Steel KP, Libby RT, Kendrick-Jones J, Buss F (2003) Loss of myosin VI reduces secretion and the size of the Golgi in fibroblasts from Snell's waltzer mice. EMBO J 22: 569-579

Wells AL, Lin AW, Chen LQ, Safer D, Cain SM, Hasson T, Carragher BO, Milligan RA, Sweeney HL (1999) Myosin VI is an actin-based motor that moves backwards. Nature 401:505-508

Figure legends

Fig. 1 Ultrastructure of individualizing actin cones. Different important details of the actin cones' ultrastructure were visualized in longitudinal sections of actin cones decorated with myosin II S1 subfragment (**a-b**) and fixed using a standard fixation procedure for conventional EM (**c-d**). The cones shown in **b** and **d** are at a later stage than the cones shown in **a** and **c**. Large *arrow* in **c** indicates the direction of the cones' movement, small *arrows* in **c** indicate the membrane connecting neighboring cones, and *arrow-heads* on **c** and **d** indicate the individual spermatid membrane; *ax*, axoneme; *mi*, mitochondria. *Bars* 1 μm.

Fig. 2 Post-embedding immunogold localization of actin in the cones; **b** is a higher magnification of the *insert* (**i**) marked on **a**. Large *arrow* in **a** indicates the direction of the cones movement, small *arrows* indicate the individual cone membrane (**a**) and actin labeling adjacent to the cone membrane (**b**); ax, *axoneme*; mi, *mitochondria*. *Bars* 1 μm (**a**) and 200 nm (**b**).

Fig. 3 Standard pre-embedding immunogold localization of actin in the cones; **b** and **c** are higher magnifications of the *inserts* (**i** and **ii**, respectively) marked on **a**. Large *arrow* in **a** indicates the direction on the cone movement, small *arrows* in **a** indicate some empty spaces where actin filaments were destroyed during sample preparation; ax, *axoneme*; mi, *mitochondria*. *Bars* 1 μm (**a**) and 200 nm (**b-c**).

Fig. 4 Modified pre-embedding immunogold localization of actin in the cones. Large *arrow* in **a** indicates the direction on the cone movement, small *arrows* in **c** indicate actin labeling adjacent to the cone membrane; ax, *axoneme*; mi, *mitochondria*. *Bars* 1 μm (**a-b**) and 200 nm (**c**).

16

Fig. 5 Double labeling of myosin VI and actin in the actin cones at the light microscope level. Myosin VI immunolocalization is in green and actin phalloidin staining is in red. *Bars* 10 μm.

Fig. 6 Modified pre-embedding immunogold localization of myosin VI in the actin cones. The cone shown in **a** is at an earlier stage than the cones shown in **b-c**. Large *arrow* in **a** indicates the direction on the cones movement, small *arrows* in **b** indicate myosin VI concentrated at the extreme edge of the actin cone front domain, and double arrows in **b-c** indicate the membrane connecting neighboring cones. Control section (**d**) did not reveal any specific labeling within the actin structures, except for a few randomly distributed background particles; ax, *axoneme*; mi, *mitochondria*. *Bars* 1 μm (**a**, **d**) and 200 nm (**b-c**).
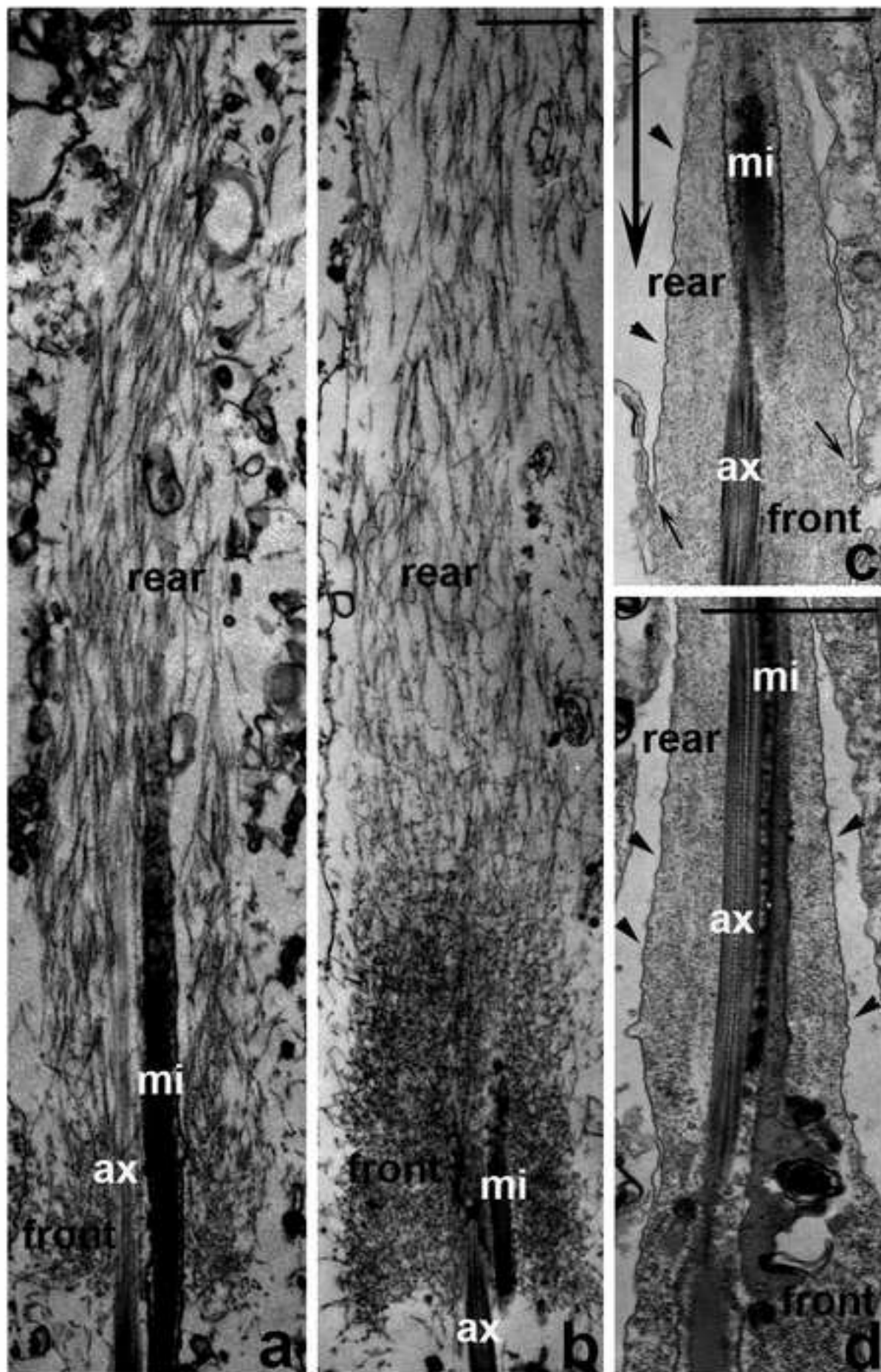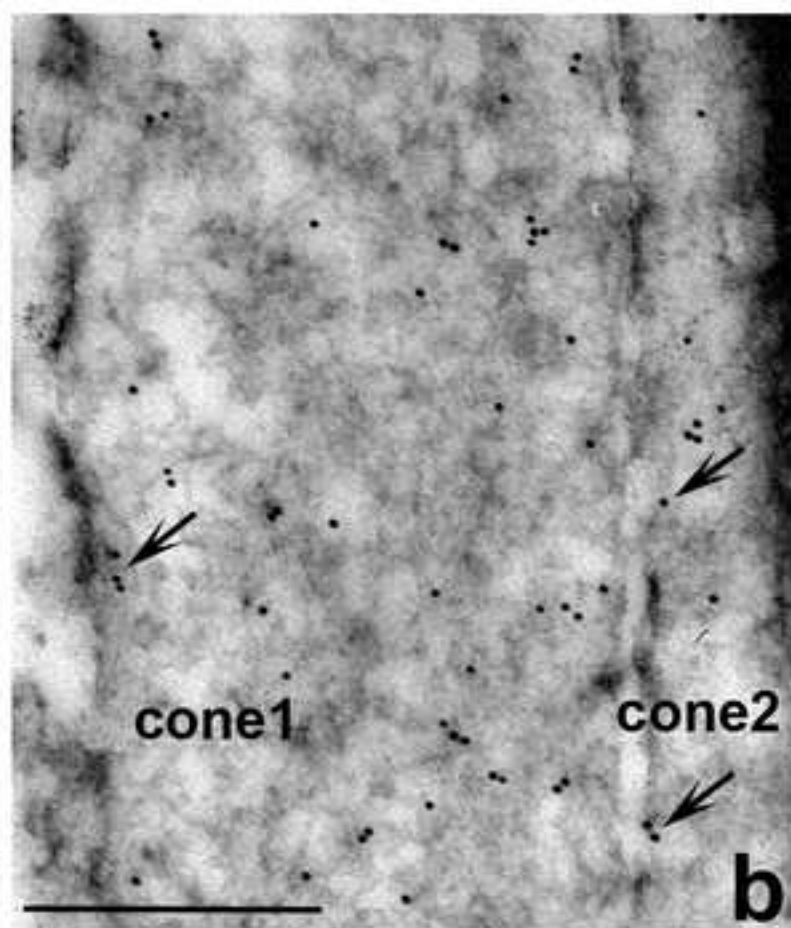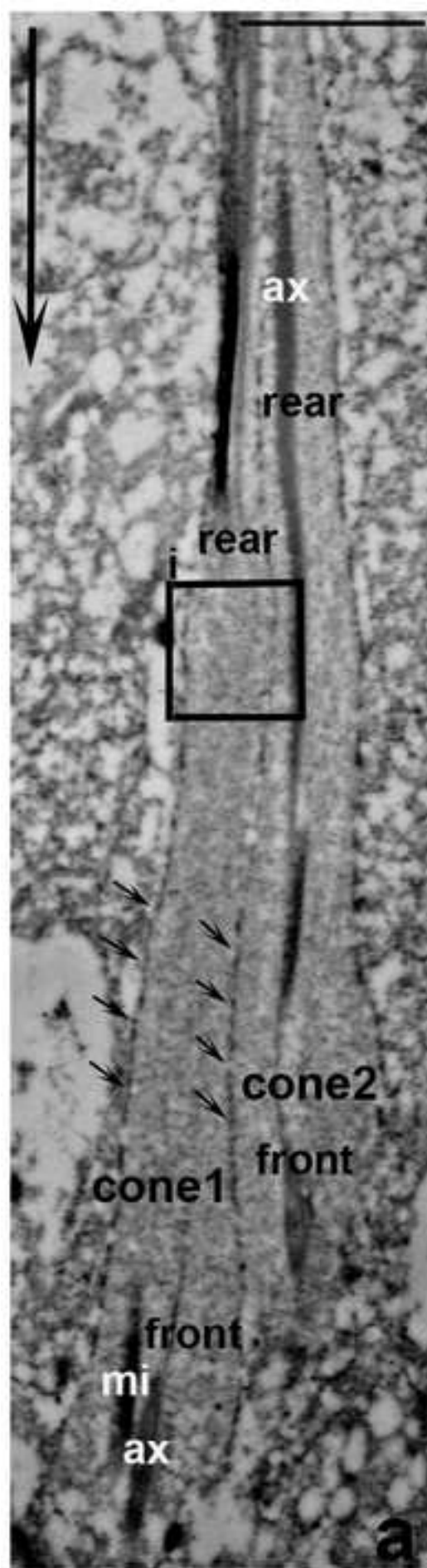
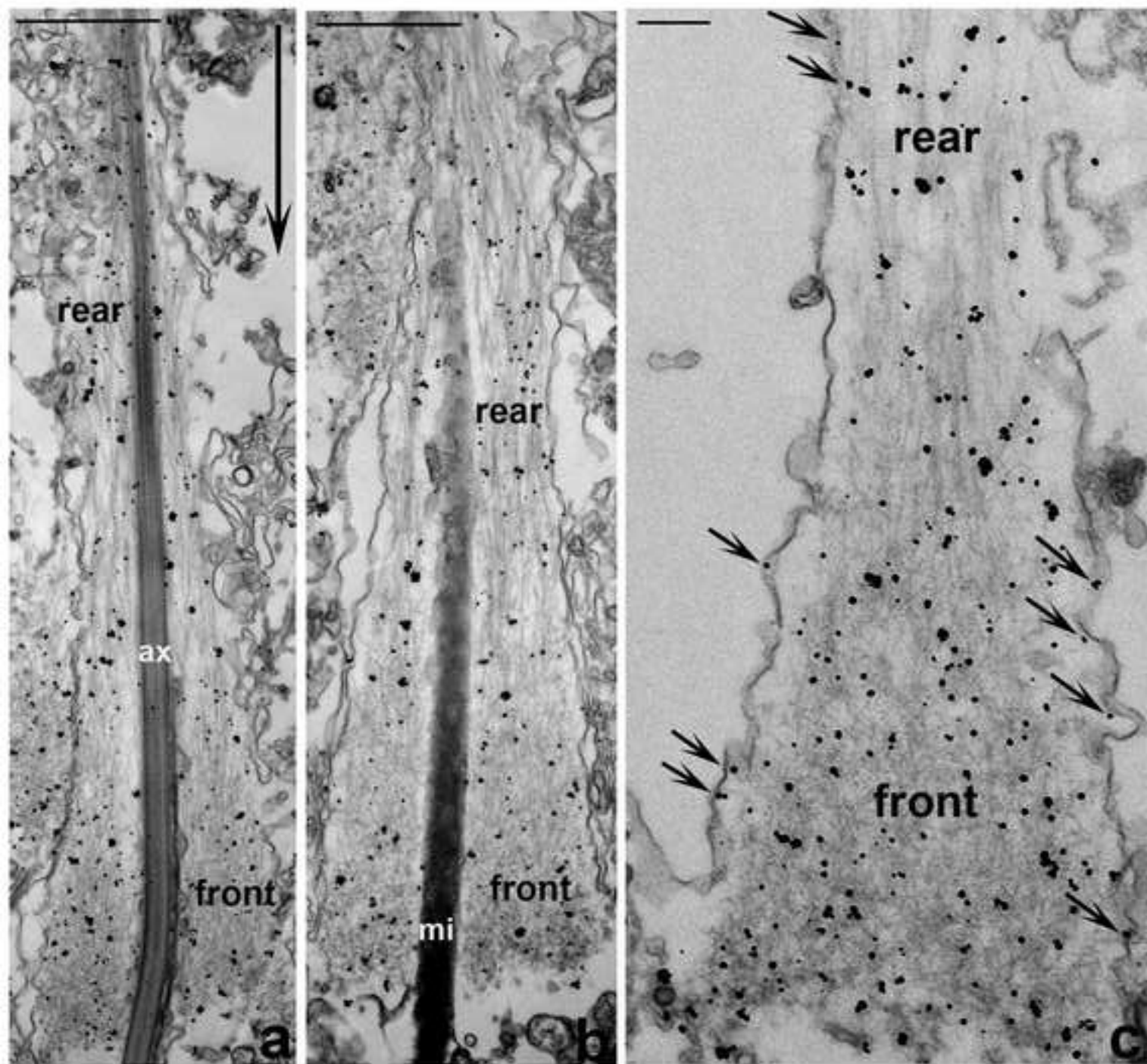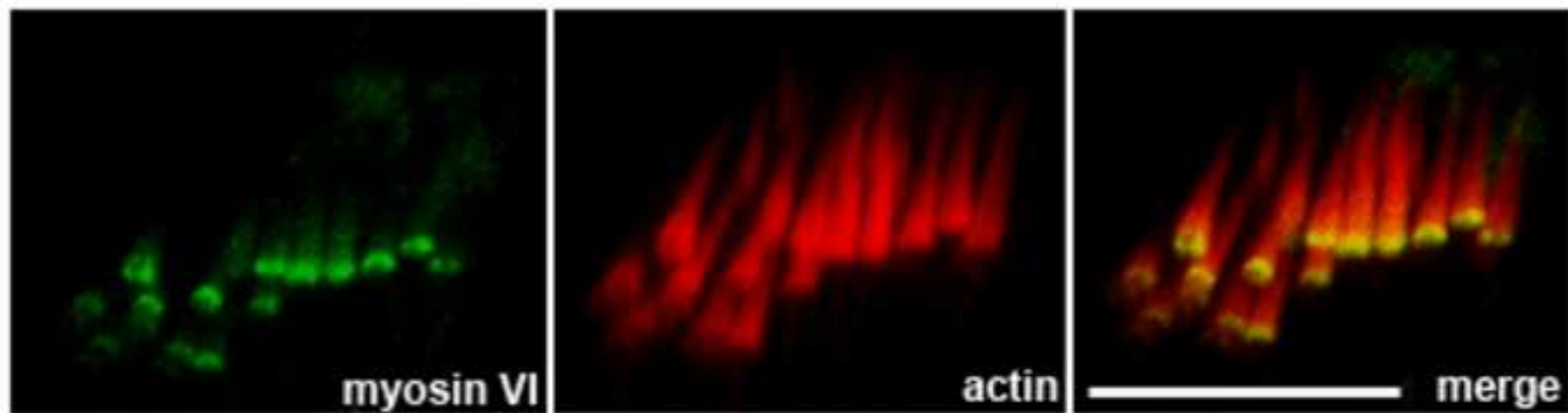**Figure 3**
Click here to download high resolution image
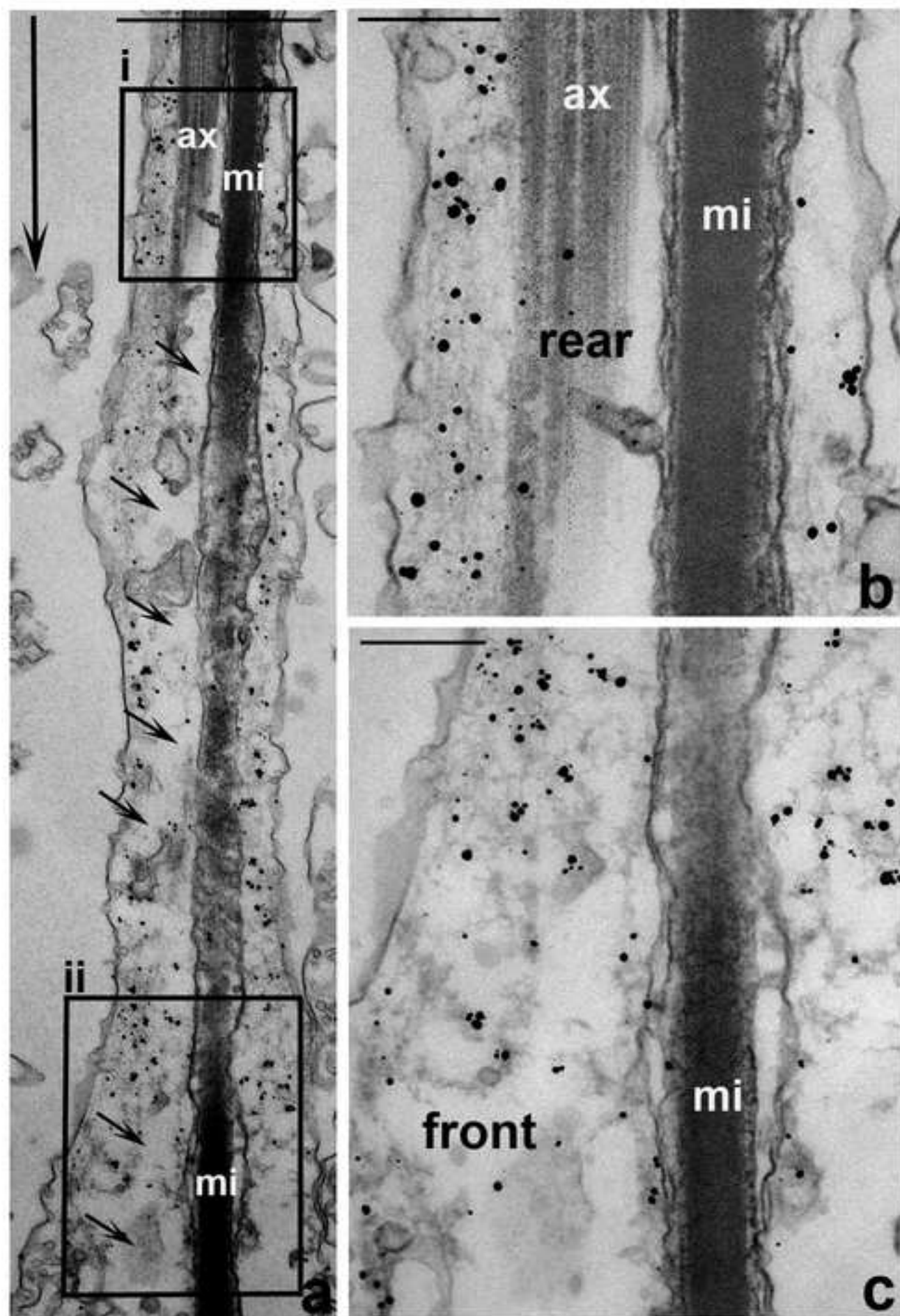
Figure 4
Click here to download high resolution image

Figure 5